

Discovery and Preclinical Evaluation of BMS-986242, a Potent, Selective Inhibitor of Indoleamine-2,3-dioxygenase 1

Emily C. Cherney,* Liping Zhang, Susheel Nara, Xiao Zhu, Johnni Gullo-Brown, Derrick Maley, Tai-An Lin, John T. Hunt, Christine Huang, Zheng Yang, Celia Darienzo, Lorell Discenza, Asoka Ranasinghe, Mary Grubb, Theresa Ziemba, Sarah C. Traeger, Xin Li, Kathy Johnston, Lisa Kopcho, Mark Fereshteh, Kimberly Foster, Kevin Stefanski, Joseph Fargnoli, Jesse Swanson, Jennifer Brown, Diane Delpy, Steven P. Seitz, Robert Borzilleri, Gregory Vite, and Aaron Balog

Cite This: *ACS Med. Chem. Lett.* 2021, 12, 288–294

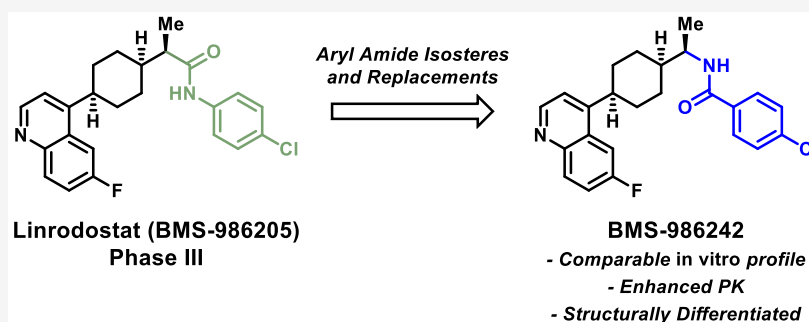
Read Online

ACCESS |

Metrics & More

Article Recommendations

Supporting Information



ABSTRACT: Indoleamine 2,3-dioxygenase 1 (IDO1) is a heme-containing dioxygenase enzyme implicated in cancer immune response. This account details the discovery of BMS-986242, a novel IDO1 inhibitor designed for the treatment of a variety of cancers including metastatic melanoma and renal cell carcinoma. Given the substantial interest around this target for cancer immunotherapy, we sought to identify a structurally differentiated clinical candidate that performs comparably to linrodostat (BMS-986205) in terms of both *in vitro* potency and *in vivo* pharmacodynamic effect in a mouse xenograft model. On the basis of its preclinical profile, BMS-986242 was selected as a candidate for clinical development.

KEYWORDS: indoleamine 2,3-dioxygenase, IDO1, BMS-986242, immuno-oncology

Human indoleamine 2,3-dioxygenase 1 (IDO1) metabolizes the essential amino acid L-tryptophan (L-trp) into kynurenine via N-formylkynurenine and is expressed in tumor-associated cells such as dendritic cells (DCs) and endothelial cells, as well as tumor cells themselves.¹ High levels of IDO1 expression in tumors or draining lymph nodes is a negative prognostic factor for several tumor types including melanoma, colon cancer, brain tumors, ovarian cancer, acute myelogenous leukemia, and others.² IDO1 expression is upregulated by type I and type II interferons, COX-2 via PGE2 production, and reverse signaling from inhibitory T cell coreceptors including cytotoxic T-lymphocyte-associated protein 4 (CTLA-4) binding to CD80 on DCs.¹ Furthermore, IDO1 has been implicated in immune escape in the tumor microenvironment, and inhibition of IDO1 has been shown to counter this effect.³ Many cancer immunotherapies aim to activate T cells within the tumor microenvironment or cause antitumor inflammation which can, itself, induce IDO1 expression. Consequently, these

immunotherapies may be increasingly effective when administered in combination with an IDO1 inhibitor.⁴

IDO1 potentiates a variety of effector pathways. Elevated levels of IDO1 in the tumor microenvironment can cause local depletion of L-trp leading to immune tolerance of tumoral antigens.⁵ Specifically, local L-trp depletion may cause stress response kinase general control nonderepressible 2 (GCN2) activation.⁶ Activation of GCN2 can bias differentiation of naive T cells into T_{reg} cells, cause T cell anergy, and inhibit T cell proliferation.⁷ GCN2 can also alter the phenotype of DCs to produce IL-10, transforming growth factor beta (TGFβ) and other inhibitory cytokines.⁸ L-trp depletion may also cause master amino acid-sensing kinase

Received: December 20, 2020

Accepted: January 22, 2021

Published: January 28, 2021



glucokinase-1 (GLK1) blockade leading to mammalian target of rapamycin complex 1 (mTORC1) and protein kinase C theta (PKC- θ) inhibition.⁹ Kynurenine produced by IDO1 binds and activates the aryl hydrocarbon receptor (AhR), which encourages T_{reg} differentiation and the formation of DCs with an immunosuppressive phenotype.¹⁰

IDO1 is a monomeric heme-containing enzyme that catalyzes the initial, rate-limiting step of L-tryptophan catabolism. Specifically, IDO1 catalyzes pyrrole ring cleavage in D- or L-tryptophan by incorporating both atoms of molecular oxygen (O₂) to form N-formyl kynurenine and subsequently kynurenine.¹¹ Other enzymes capable of affecting this transformation include IDO2 and tryptophan 2,3-dioxygenase (TDO). In contrast to IDO1, TDO is tetrameric, enantiospecific (will only catalyze the cleavage of L-tryptophan) and constitutively expressed in the liver and brain.¹² TDO is primarily responsible for regulating systemic L-tryptophan levels suggesting that its role may be distinct from IDO1.¹³ Less is known about IDO2; however, it has 43% sequence homology with IDO1 and reduced affinity for L-tryptophan, implying decreased activity.¹⁴

Dozens of IDO1 inhibitors have been reported and assessed preclinically, while several others have been clinically investigated in combination with chemotherapeutics, checkpoint inhibitors, and vaccines.¹⁵ The structures of several of these clinical candidates, including linrodostat mesylate (BMS-986205) (1),^{16a} epacadostat (2),^{16b} indoximod (3),^{16c} navoximod (4),^{16d} and PF06840003 (5),^{16e} are shown in Figure 1. While clinical trials with various IDO1

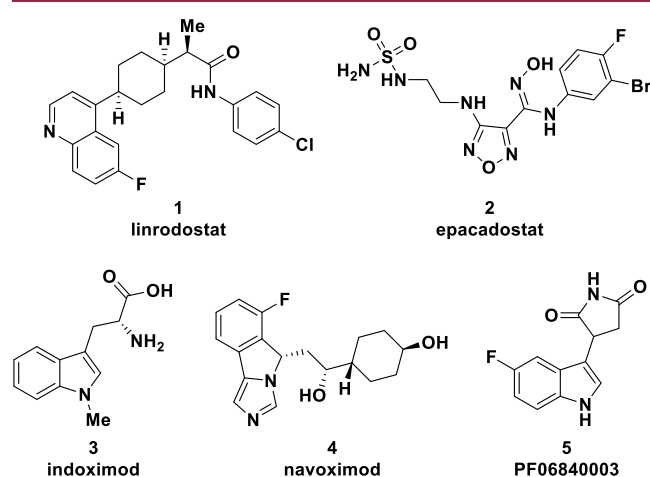


Figure 1. Clinically investigated IDO1 inhibitors.

inhibitors have been terminated because of lack of clinical response,¹⁷ it has become clear that different IDO1 inhibitors are acting through several discrete mechanisms which could impact pharmacology and clinical outcomes.¹⁸ Moreover, linrodostat has a unique mechanism of inhibition targeting apo-IDO1 in contrast to other clinically assessed IDO1 inhibitors (see Figure 1) which likely target holo-IDO1.¹⁹

Previously, the discovery of linrodostat (1), a heme displacing, cyclohexyl quinoline IDO1 inhibitor, was disclosed.^{16a} This compound demonstrated potent human IDO1 inhibitory activity in HeLa cells and human whole blood that compared favorably with competitor compounds. Currently, linrodostat is in several clinical trials including a phase III study in bladder cancer in combination with nivolumab, as

well as phase I and II studies in a variety of tumor types.²⁰ Herein, we will discuss efforts to find a structurally differentiated IDO1 inhibitor resulting in the identification of BMS-986242, which possesses a preclinical PK/PD profile comparable to linrodostat.

An X-ray cocrystal structure of compound 6 (a closely related analogue of BMS-986205) was utilized in the design of new IDO1 inhibitors (Figure 2).^{19a} The key interaction

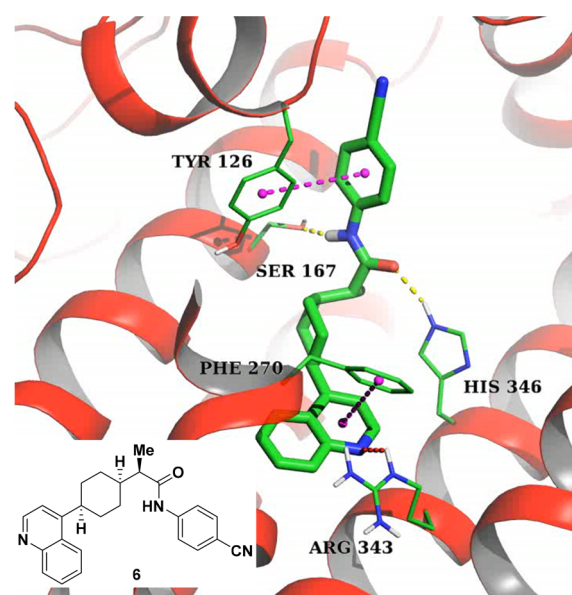
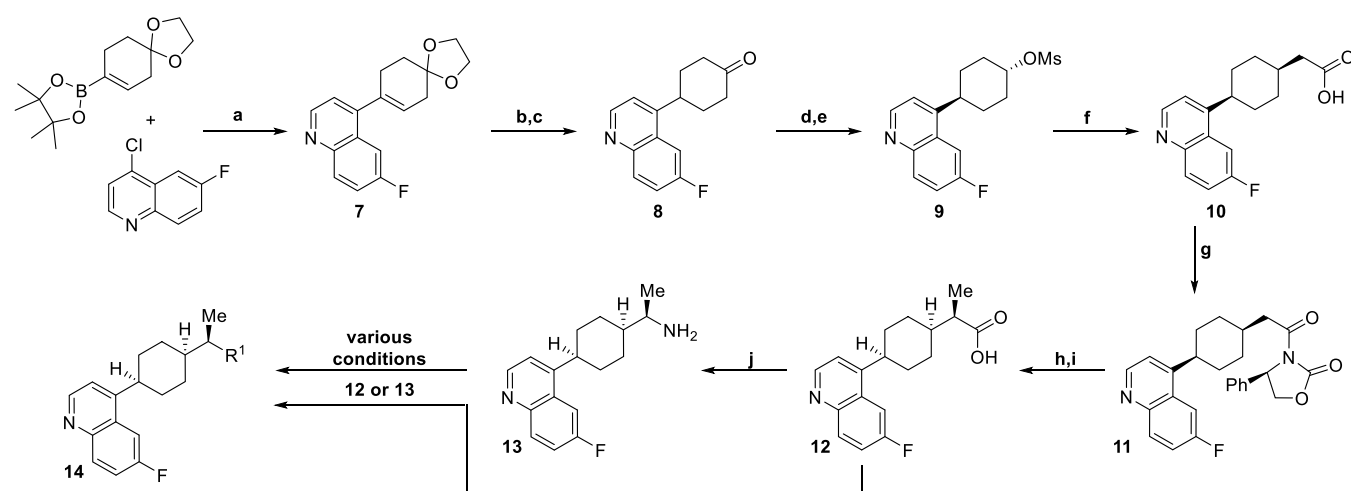


Figure 2. Crystal structure of compound 6 bound to hIDO1.

involves hydrogen bonding between the NH of the amide bond and Ser167 as well as the amide carbonyl and His346. There is also a potential hydrogen bonding event between the nitrogen of the quinoline and Arg343. Additionally, the crystal reveals edge to face pi stacking interactions between the cyanophenyl group and Tyr126 as well as between the quinoline ring and Phe270. When the pursuit to identify a structurally differentiated clinical candidate began, we were aware that the aryl amide-containing region of linrodostat was tolerant of a variety of modifications, so we chose to focus our efforts on this portion of the molecule first.

Expedient exploration of a diverse range of aryl amide isosteres and replacements necessitated a synthetic route wherein the key intermediate would already contain the cyclohexyl-quinoline core with all stereochemistry set. To achieve this, new compounds of generic structure 14 were prepared according to the sequence outlined in Scheme 1 via intermediates 12 or 13. To begin, a previously reported vinyl boronic acid²¹ was coupled to commercially available 4-chloro-6-fluoroquinoline under standard Suzuki coupling conditions to provide 7. Hydrogenation of 7 with Degussa-type palladium was necessary to avoid over reduction of the quinoline. Subsequent hydrolysis of the ketal gave ketone 8. Diastereoselective reduction of the resulting ketone with sodium borohydride preferentially gave the *trans*-alcohol (in a 5:1 *trans*–*cis* ratio) which was then mesylated to yield 9. Next, a one-pot process involving mesylate displacement with di-*tert*-butyl malonate followed by acetic acid mediated *tert*-butyl group deprotection with concomitant decarboxylation provided *cis*-acid 10 containing the necessary stereochemistry around the cyclohexyl ring. The α -methyl group of the acid

Scheme 1. Synthetic Route to Cyclohexyl Quinolines^a

^aReagents and conditions: a. Pd(PPh₃)₄, K₂CO₃, dioxane, water, 100 °C, 16 h (77%); b. Pd/C (Degussa), NH₄HCO₂; c. 4 M HCl, Acetone (75% over 2 steps); d. NaBH₄ (5:1 *trans:cis* dr); e. MsCl, Pyr. (76% over 2 steps); f. (i) NaH, di-*t*Bu-malonate, (ii) AcOH, 130 °C (76%); g. PivCl, TEA; lithium-*(R)*-2-oxo-4-phenyloxazolidin-3-ide (85%); h. NaHMDS, -40 °C; MeI (>20:1 dr) (68%); i. LiOH, H₂O₂ (82%); j. DPPA, TEA; LiOH, H₂O (90%)

was installed stereoselectively using an Evan's oxazolidinone chiral auxiliary. Alkylation of oxazolidinone-containing intermediate **11** with methyl iodide allowed for installation of the methyl group in >20:1 diastereoselectivity in favor of the desired diastereomer. Cleavage of the chiral auxiliary led to intermediate **12**. This intermediate could lead to a variety of amide replacements or isosteres using procedures outlined in the Supporting Information provided, as well as other variations not disclosed in this manuscript but exemplified elsewhere.²² Alternatively, this intermediate (**12**) could be converted to amine **13** via Curtius rearrangement to give another intermediate useful for introducing diversity.²² From intermediates **12** and **13**, a variety of amide isosteres and replacements were synthesized (compounds **15**–**25**) (see Supporting Information for details) and assessed in both human HeLa and murine M109 cellular IDO1 inhibition assays where IDO activity can be induced upon treatment with IFN γ as well as a human whole blood (HWB) IDO1 inhibition assay (Table 1).

We initiated our efforts by synthesizing compounds such as pyrimidine **15**, benzylamine **16**, and cyclohexylamine **17**. While heterocycles, such as pyrimidine **15**, were tolerated in several cases (not shown),²² none were as potent as compound **1**, and all showed inferior HWB potency. Benzylamines (like **16**) and primary aliphatic amines (not shown) were generally not well tolerated. Of the aliphatic amines explored, cyclohexylamine **17** was the most successful; however, this compound had very poor HWB activity and metabolic stability. Removing the carbonyl group in **1** led to analogue **18**. While **18** did maintain a decent level of potency (within ~3-fold of **1**) in the human cellular and whole blood assays, it was >10-fold less potent in the murine M109 cellular assay. Moving the nitrogen over one position as in compound **19** rendered compound **19** significantly less active. Several heterocyclic isosteres were tolerated including benzimidazole **20** which was only 2-fold less potent than **1** in the HeLa and HWB assays. Further exploration of heterocyclic isosteres will be the topic of a future publication. Sulfonamides such as **21** were found to be inactive and

although ureas (**22**) were able to maintain some potency, mediocre HWB potency made them implausible candidates. Finally, several “reverse” amides were synthesized. Two homologated analogues containing four-atom linkers between the cyclohexyl core and the *p*-chlorophenyl ring (**23** and **24**) were much less potent than **1** across assay types. In contrast, the “reverse” amide analogue **25** that possessed a three-atom linker between the cyclohexyl core and the *p*-chlorophenyl ring displayed the same level of cellular potency and was within 2-fold of the HWB potency of linrodostat (**1**). On the basis of this promising result, SAR around the “reverse” amides was surveyed (Table 2).

Synthesis of the *meta*-chloro (**26**) and *ortho*-chloro (**27**) versions of compound **25** revealed an advantage for *para*-substitution on the phenyl ring both in terms of potency and metabolic stability. Aliphatic reverse amides like **28** and **29** again maintained decent (<25 nM in HeLa) human cellular potency like their “forward” amide versions (i.e., **17**), but also suffered from poor HWB activity and metabolic stability. The *para*-biphenyl analogue **30** had an overall superior *in vitro* profile based on potency and metabolic stability; however, this compound suffered from extremely poor solubility (<0.001 mg/mL at pH 7.4 and 6.5) and was consequently not progressed. In the course of our efforts to improve the solubility of these compounds, we also found that a wide variety of polar functionalities were tolerated at the *meta*-position as exemplified by compound **31**. Based on the cocrystal structure of **6** shown above, we believe that these polar groups are projecting out of the binding pocket and may be solvent exposed. Unfortunately, molecules like **31** did not improve aqueous solubility (still <0.001 mg/mL at 6.5) and most had very poor metabolic stability. On the basis of this data, “reverse” amide **25** (which was assigned as BMS-986242) was profiled more extensively both *in vitro* and *in vivo*.

Further *in vitro* ADMET profiling (Table 3) revealed that BMS-986242 was more prone to oxidative metabolism and less susceptible to glucuronidation. Biotransformation studies in hepatocytes across species (H, M, R, D, C) identified

Table 1. SAR of Amide Isosteres and Replacements

Cmpd #	R ¹	HeLa/M109 IC ₅₀ (nM) ^a	HWB IC ₅₀ (nM) ^b	HLM/MsLM ^c
1		2/5	9	84/31
15		10/92	80	73/51
16		67/870	>1000	19/5
17		18/287	470	<1/<1
18		7/62	44	80/80
19		745/>1000	>1000	34/2
20		4/12	28	48/12
21		>1000/>1000	484	29/<1
22		20/67	280	52/14
23		125/651	779	8/2
24		261/772	158	56/32
25 BMS-986242		2/2	25	54/21

^aData reported as average of ≥ 3 test results. See [Supporting Information](#) for description of assay conditions. ^bData reported as average of ≥ 2 test results. See [Supporting Information](#) for description of assay conditions. ^cPercentage of the parent compound (0.5 μ M) remaining after a 10 min incubation with 1 mg/mL of HLM or MsLM.

several oxidative metabolites as well as metabolites where the resulting oxygen was capped as the glucuronide; however, no direct glucuronidation of the parent molecule was observed. Several oxidative metabolites were identified and profiled. They were found to be substantially less potent (>200 nM) than parent in the HWB assay. Intrinsic permeability was satisfactory, and the compound does have a moderate potential for drug–drug interactions based upon CYP inhibition of 2C8, 2C9 and 2C19. While compound BMS-986242 showed 87% hERG inhibition and <20% sodium channel inhibition in a patch clamp assay at a 10 μ M concentration at both 1 and 4 Hz, it was also highly protein bound which mitigates this liability. Additionally, no adverse findings were observed in a rat CV telemetry study. In an *in vitro* safety panel consisting of 40 targets, BMS-986242 showed IC₅₀ > 25 μ M for all targets except nAChR $\alpha 1$ (IC₅₀ = 12.3 μ M) and nAChR $\alpha 7$ (IC₅₀ > 6 μ M with ~20% max inhibition). The pharmacokinetics of BMS-986242 were investigated in mice, rats, dogs, and monkeys (see [Table 4](#)). Despite a seemingly poor *in vitro* oxidative metabolic

Table 2. “Reverse” Amide SAR

Cmpd #	R ¹	HeLa/M109 IC ₅₀ (nM) ^a	HWB IC ₅₀ (nM) ^b	HLM/MsLM ^c
26		7/48	97	39/9
27		12/215	135	21/7
28		24/56	579	9/10
29		12/86	294	6/5
30		2/3	22	59/70
31		7/20	35	2/4

^aData reported as average of ≥ 3 test results. See [Supporting Information](#) for description of assay conditions. ^bData reported as average of ≥ 2 test results. See [Supporting Information](#) for description of assay conditions. ^cPercentage of the parent compound (0.5 μ M) remaining after a 10 min incubation with 1 mg/mL of HLM or MsLM.

Table 3. *In Vitro* ADMET Profile of BMS-986242 (25)

parameter	BMS-986242 (25)
met. stability CYP ($T_{1/2}$ min)	14 (H), 4 (M), 10 (R), 10 (D), 2 (C)
met. stability UGT ($T_{1/2}$ min)	>120 (H), >120 (M), 93 (R), 33 (D), >120 (C)
PAMPA (pH 7.4)	2830 nm/sec
Caco (a-b:b-a)	88:55 nm/sec
human CYP IC ₅₀ (μ M)	2C8:1.39; 2C9:0.74; 2C19:3.37; others >15
hERG patch clamp	87% inh at 10 μ M
Na ⁺ patch clamp	<20% inh at 10 μ M (1 and 4 Hz)
Ca ²⁺ patch clamp IC ₅₀	>25 μ M
protein binding (% free): h, m	<0.3, <0.2
PXR-TA EC ₅₀	>50 μ M

Table 4. Pharmacokinetic Parameters for BMS-986242 (25)

parameter	mouse ^a	rat ^a	dog ^a	cyno ^a
dose (mg/kg) iv/po	0.5 ^b /6 ^c	0.5 ^b /2 ^c	1 ^b /5 ^c	1 ^b /5 ^c
CL (mL/min/kg) iv	30	3.70	5.1	12
V _{ss} (L/kg) iv	17	0.97	3.87	1
AUC _{total} (μ M·h) iv/po	0.69/12.6	5.6/28.2	8.7/17.4	3.4/7.1
$t_{1/2}$ (h) iv	8	4	19	2
F_{po} (%)	152	127	39	42

^aData reported as average of ≥ 3 animals. ^b70% PEG 400; 30% water. ^c5% ethanol; 55% PEG 400; 20% propylene glycol; 20% TPGR.

stability profile, BMS-986242 had a suitable PK profile across species. Oral bioavailability was $\geq 39\%$ in all tested species.

Pharmacodynamic effects were studied in a nu/nu mouse xenograft model: mice were implanted with SKOV3 cells (human ovarian cancer cell line) 2 weeks prior to treatment (see [Table 5](#) for results, see [Supporting Information](#) for protocol details). Compound exposure in the tumor was then monitored (PK), and pharmacodynamic (PD) effects were

Table 5. PK–PD Study of BMS-986242 (25) vs Linrodostat vs Epacadostat in Human SKOV3 Xenograft Tumor Mouse Model

compound	dose (mg/kg)	PK ^a	PD ^b
BMS-986242 (25)	3 ^c	9.6	45%
BMS-986242 (25)	10 ^c	21.1	58%
BMS-986242 (25)	30 ^c	61.0	59%
linrodostat (1)	60 ^c	34.9	61%
epacadostat (2)	100 ^d	48.0	54%

^aPK is AUC (0–24 h) in $\mu\text{M}^*\text{h}$ measured in the tumor. ^bPD is percent kynurenine AUEC (0–24 h) reduction measured in the tumor. %Kyn reduction was measured at steady state after the 5th dose, calculated as the area under Kyn concentration–time curve from 0 to 24 h and compared with that of vehicle control. ^cQD PO dosing. ^dBID PO dosing.

quantified by observing kynurenine (a downstream product of tryptophan metabolism catalyzed by IDO1) levels in the tumor. BMS-986242 (3, 10, and 30 mpk QD PO), linrodostat (60 mpk QD PO), and epacadostat (100 mpk BID PO) were all examined in this mouse xenograft model. BMS-986242 (25) exhibited dose-proportional exposure and a statistically significant reduction in kynurenine concentration in the tumor at all three doses. In this model, the pharmacodynamic effect of a 10 mpk QD dose of BMS-986242 (25) was comparable to a 60 mpk QD dose of linrodostat (1) and a 100 mpk BID dose of epacadostat (2) despite having lower levels of exposure (21.1 vs 34.9 vs 48.0 $\mu\text{M}^*\text{h}$, respectively). Also of note, the 30 mpk dose of BMS-986242 provided significantly higher levels of exposure than the 60 mpk dose of linrodostat (60.1 vs 34.9 $\mu\text{M}^*\text{h}$ respectively)

In summary, we have identified BMS-986242 (25) as a structurally differentiated clinical candidate for IDO1 inhibition with robust human and mouse *in vitro* activity as well as dose proportional exposure and significant PD effect *in vivo* in a mouse xenograft model. BMS-986242 elicited a PD effect comparable to linrodostat (1) and epacadostat (2) in a PD model of tumor kynurenine reduction at a lower level of exposure. Given the promising preclinical safety and pharmacodynamic profile of BMS-986242, it was progressed into a phase I/II study in combination with nivolumab.²³

■ ASSOCIATED CONTENT

Supporting Information

The Supporting Information is available free of charge at <https://pubs.acs.org/doi/10.1021/acsmchemlett.0c00668>.

Biological assays, pharmacokinetic studies, *in vivo* pharmacokinetic-pharmacodynamic study, experimental procedures, and analytical data for key compounds (PDF)

■ AUTHOR INFORMATION

Corresponding Author

Emily C. Cherney – Bristol Myers Squibb Research and Development, Lawrence Township, New Jersey 08648, United States; orcid.org/0000-0003-1977-2900; Email: emily.cherney@bms.com

Authors

Liping Zhang – Bristol Myers Squibb Research and Development, Lawrence Township, New Jersey 08648, United States; orcid.org/0000-0002-1797-7227

Susheel Nara – Biocon BMS R&D Center, Bengaluru, Karnataka 560099, India

Xiao Zhu – Bristol Myers Squibb Research and Development, Lawrence Township, New Jersey 08648, United States; orcid.org/0000-0001-7647-4390

Johnni Gullo-Brown – Bristol Myers Squibb Research and Development, Lawrence Township, New Jersey 08648, United States

Derrick Maley – Bristol Myers Squibb Research and Development, Lawrence Township, New Jersey 08648, United States

Tai-An Lin – Bristol Myers Squibb Research and Development, Lawrence Township, New Jersey 08648, United States

John T. Hunt – Bristol Myers Squibb Research and Development, Lawrence Township, New Jersey 08648, United States

Christine Huang – Bristol Myers Squibb Research and Development, Lawrence Township, New Jersey 08648, United States

Zheng Yang – Bristol Myers Squibb Research and Development, Lawrence Township, New Jersey 08648, United States

Celia Darienzo – Bristol Myers Squibb Research and Development, Lawrence Township, New Jersey 08648, United States

Lorell Discenza – Bristol Myers Squibb Research and Development, Lawrence Township, New Jersey 08648, United States

Asoka Ranasinghe – Bristol Myers Squibb Research and Development, Lawrence Township, New Jersey 08648, United States

Mary Grubb – Bristol Myers Squibb Research and Development, Lawrence Township, New Jersey 08648, United States

Theresa Ziemba – Bristol Myers Squibb Research and Development, Lawrence Township, New Jersey 08648, United States

Sarah C. Traeger – Bristol Myers Squibb Research and Development, Lawrence Township, New Jersey 08648, United States

Xin Li – Bristol Myers Squibb Research and Development, Lawrence Township, New Jersey 08648, United States

Kathy Johnston – Bristol Myers Squibb Research and Development, Lawrence Township, New Jersey 08648, United States

Lisa Kopcho – Bristol Myers Squibb Research and Development, Lawrence Township, New Jersey 08648, United States

Mark Fereshteh – Bristol Myers Squibb Research and Development, Lawrence Township, New Jersey 08648, United States

Kimberly Foster – Bristol Myers Squibb Research and Development, Lawrence Township, New Jersey 08648, United States

Kevin Stefanski – Bristol Myers Squibb Research and Development, Lawrence Township, New Jersey 08648, United States

Joseph Fargnoli – Bristol Myers Squibb Research and Development, Lawrence Township, New Jersey 08648, United States

Jesse Swanson – Bristol Myers Squibb Research and Development, Lawrence Township, New Jersey 08648, United States

Jennifer Brown – Bristol Myers Squibb Research and Development, Lawrence Township, New Jersey 08648, United States

Diane Delpy – Bristol Myers Squibb Research and Development, Lawrence Township, New Jersey 08648, United States

Steven P. Seitz – Bristol Myers Squibb Research and Development, Lawrence Township, New Jersey 08648, United States

Robert Borzilleri – Bristol Myers Squibb Research and Development, Lawrence Township, New Jersey 08648, United States

Gregory Vite – Bristol Myers Squibb Research and Development, Lawrence Township, New Jersey 08648, United States

Aaron Balog – Bristol Myers Squibb Research and Development, Lawrence Township, New Jersey 08648, United States

Complete contact information is available at:
<https://pubs.acs.org/10.1021/acsmchemlett.0c00668>

Author Contributions

The manuscript was written through contributions of all authors. All authors have given approval to the final version of the manuscript.

Notes

The authors declare no competing financial interest.

REFERENCES

- (1) Katz, J. B.; Muller, A. J.; Prendergast, G. C. Indoleamine 2,3-dioxygenase in T-cell tolerance and tumoral immune escape. *Immunol. Rev.* **2008**, *222*, 206–221.
- (2) (a) Munn, D. H.; Sharma, M. D.; Hou, D.; Baban, B.; Lee, J. R.; Antonia, S. J.; Messina, J. L.; Chandler, P.; Koni, P. A.; Mellor, A. J. Expression of indoleamine 2,3-dioxygenase by plasmacytoid dendritic cells in tumor-draining lymph nodes. *J. Clin. Invest.* **2004**, *114*, 280–290. (b) Gerlini, G.; Di Gennaro, P.; Mariotti, G.; Urso, C.; Chiarugi, A.; Pimpinelli, N.; Borgognoni, L. Indoleamine 2,3-dioxygenase⁺ cells correspond to the BDCA2⁺ plasmacytoid dendritic cells in human melanoma sentinel nodes. *J. Invest. Dermatol.* **2010**, *130*, 898–901. (c) Speckaert, R.; Vermaelen, K.; van Geel, N.; Autier, P.; Lambert, J.; Haspelslagh, M.; Van Gele, M.; Thielemans, K.; Neyns, B.; Roche, N.; Verbeke, N.; Deron, P.; Speckaert, M.; Brochez, L. Indoleamine 2,3-dioxygenase, a new prognostic marker in sentinel lymph nodes of melanoma patients. *Eur. J. Cancer* **2012**, *48*, 2004–2011. (d) Ferdinande, L.; Decaestecker, C.; Verset, L.; Mathieu, A.; Moles Lopez, X.; Negulescu, A. M.; Van Maerken, T.; Salmon, L.; Cuvelier, C. A.; Demetter, P. Clinicopathological significance of indoleamine 2,3-dioxygenase 1 expression in colorectal cancer. *Br. J. Cancer* **2012**, *106*, 141–147. (e) Brandacher, G.; Perathoner, A.; Ladurner, R.; Schneeberger, S.; Obrist, P.; Winkler, C.; Werner, E. R.; Werner-Felmayer, G.; Weiss, H. G.; Göbel, G.; Margreiter, R.; Königsrainer, A.; Fuchs, D.; Amberger, A. Prognostic value of indoleamine 2,3-dioxygenase expression in colorectal cancer: effect on tumor-infiltrating T cells. *Clin. Cancer Res.* **2006**, *12*, 1144–1151. (f) Zhai, L.; Lauing, K. L.; Chang, A. L.; Dey, M.; Qian, J.; Cheng, Y.; Lesniak, M. S.; Wainwright, D. A. The role of IDO in brain tumor immunotherapy. *J. Neuro-Oncol.* **2015**, *123*, 395–403.

- (g) Okamoto, A.; Nikaido, T.; Ochiai, K.; Takakura, S.; Saito, M.; Aoki, Y.; Ishii, N.; Yanaiharu, N.; Yamada, K.; Takikawa, O.; Kawaguchi, R.; Isonishi, S.; Tanaka, T.; Urashima, M. Indoleamine 2,3-dioxygenase serves as a marker of poor prognosis in gene expression profiles of serous ovarian cancer cells. *Clin. Cancer Res.* **2005**, *11*, 6030–6039. (h) Chamuleau, M. E.; Van de Loosdrecht, A. A.; Hess, C. J.; Janssen, J. J.; Zevenbergen, A.; Delwel, R.; Valk, P. J.; Löwenberg, B.; Ossenkoppele, G. J. High INDO (indoleamine 2,3-dioxygenase) mRNA level in blasts of acute myeloid leukemic patients predicts poor clinical outcome. *Haematologica* **2008**, *93*, 1894–1898. (i) Folgiero, V.; Goffredo, B. M.; Filippini, P.; Masetti, R.; Bonanno, G.; Caruso, R.; Bertaina, V.; Mastronuzzi, A.; Gaspari, S.; Zecca, M.; Torelli, G. F.; Testi, A. M.; Pession, A.; Locatelli, F.; Rutella, S. Indoleamine 2,3-dioxygenase 1 (IDO1) activity in leukemia blasts correlates with poor outcome in childhood acute myeloid leukemia. *Oncotarget* **2014**, *5*, 2052–2064.

- (3) Muller, A. J.; Malachowski, W. P.; Prendergast, G. C. Indoleamine 2,3-dioxygenase in cancer: targeting pathological immune tolerance with small-molecule inhibitors. *Expert Opin. Ther. Targets* **2005**, *9*, 831–849.

- (4) (a) Gu, T.; Rowsell-Turner, R. B.; Kilinc, M. O.; Egilmez, N. K. *Cancer Res.* **2010**, *70*, 129–138. (b) Grohmann, U.; Orabona, C.; Fallarino, F.; Vacca, C.; Calcinaro, F.; Falorni, A.; Candeloro, P.; Belladonna, M. L.; Bianchi, R.; Fioretti, M. C.; Puccetti, P. CTLA-4-Ig regulates tryptophan catabolism in vivo. *Nat. Immunol.* **2002**, *3*, 1097–1101.

- (5) Muller, A. J.; Prendergast, G. C. Indoleamine 2,3-Dioxygenase in Immune Suppression and Cancer. *Curr. Curr. Cancer Drug Targets* **2007**, *7*, 31–40.

- (6) Munn, D. H.; Sharma, M. D.; Baban, B.; Harding, H. P.; Zhang, Y.; Ron, D.; Mellor, A. L. GCN2 Kinase in T Cells Mediates Proliferative Arrest and Anergy Induction in Response to Indoleamine 2,3-Dioxygenase. *Immunity* **2005**, *22*, 633–642.

- (7) Fallarino, F.; Grohmann, U.; You, S.; McGrath, B. C.; Cavener, D. R.; Vacca, C.; Orabona, C.; Bianchi, R.; Belladonna, M. L.; Volpi, C.; Santamaria, P.; Fioretti, M. C.; Puccetti, P. The Combined Effects of Tryptophan Starvation and Tryptophan Catabolites Down-Regulate T Cell Receptor ζ -Chain and Induce a Regulatory Phenotype in Naive T Cells. *J. Immunol.* **2006**, *176*, 6752–6761.

- (8) Liu, H.; Huang, L.; Bradley, J.; Liu, K.; Bardhan, K.; Ron, D.; Mellor, A. L.; Munn, D. H.; McGaha, T. L. GCN2-Dependent Metabolic Stress Is Essential for Endotoxemic Cytokine Induction and Pathology. *Mol. Cell. Biol.* **2014**, *34*, 428–438.

- (9) Metz, R.; Rust, S.; DuHadaway, J. B.; Mautino, M. R.; Munn, D. H.; Vahanian, N. N.; Link, C. J.; Prendergast, G. C. IDO inhibits a tryptophan sufficiency signal that stimulates mTOR: A novel IDO effector pathway targeted by D-1-methyl-tryptophan. *Oncoimmunology* **2012**, *1*, 1460–1468.

- (10) (a) Quintana, F. J.; Murugaiyan, G.; Farez, M. F.; Mitsdoerffer, M.; Tukpah, A.-M.; Burns, E. J.; Weiner, H. L. An endogenous aryl hydrocarbon receptor ligand acts on dendritic cells and T cells to suppress experimental autoimmune encephalomyelitis. *Proc. Natl. Acad. Sci. U. S. A.* **2010**, *107*, 20768–20773. (b) Jaronen, M.; Quintana, F. J. Immunological relevance of the coevolution of IDO1 and AHR. *Front. Immunol.* **2014**, *5*, 521–528. (c) Manlapat, A. K.; Kahler, D. K.; Chandler, P. R.; Munn, D. H.; Mellor, A. L. Cell-autonomous control of interferon type I expression by indoleamine 2,3-dioxygenase in regulatory CD19⁺ dendritic cells. *Eur. J. Immunol.* **2007**, *37*, 1064–1071.

- (11) Sugimoto, H.; Oda, S.-I.; Otsuki, T.; Hino, T.; Yoshida, T.; Shiro, Y. Crystal structure of human indoleamine 2,3-dioxygenase: Catalytic mechanism of O₂ incorporation by a heme-containing dioxygenase. *Proc. Natl. Acad. Sci. U. S. A.* **2006**, *103*, 2611–2616.

- (12) (a) Shimizu, T.; Nomiya, S.; Hirata, F.; Hayaishi, O. Indoleamine 2,3-Dioxygenase. *J. Biol. Chem.* **1978**, *253*, 4700–4706. (b) Haber, R.; Bessette, D.; Hulihan-Giblin, B.; Durcan, M. J.; Goldman, D. Identification of Tryptophan 2,3-Dioxygenase RNA in Rodent Brain. *J. Neurochem.* **1993**, *60*, 1159–1162.

(13) (a) Greene, L. I.; Bruno, T. C.; Christenson, J. L.; D'Alessandro, A.; Culp-Hill, R.; Torkko, K.; Borges, V. F.; Slansky, J. E.; Richer, J. K. A Role for tryptophan-2,3-dioxygenase in CD8 T cell suppression and evidence of tryptophan catabolism in breast cancer patient plasma. *Mol. Cancer Res.* **2019**, *17*, 131–139. (b) Pilotte, L.; Larrieu, P.; Stroobant, V.; Colau, D.; Dolusič, E.; Fredrick, R.; De Plaen, E.; Uyttenhove, C.; Wouters, J.; Masereel, B.; Van den Eynde, B. J. Reversal of tumoral immune resistance by inhibition of tryptophan 2,3-dioxygenase. *Proc. Natl. Acad. Sci. U. S. A.* **2012**, *109*, 2497–2502. (c) Zhai, L.; Spranger, S.; Binder, D. C.; Gritsina, G.; Lauing, K. L.; Giles, F. J.; Wainwright, D. A. Molecular Pathways: Targeting IDO1 and Other Tryptophan Dioxygenases for Cancer Immunotherapy. *Clin. Cancer Res.* **2015**, *21*, 5427–5433.

(14) (a) Pantouris, G.; Serys, M.; Yuasa, H. J.; Ball, H. J.; Mowat, C. G. Human indoleamine 2,3-dioxygenase-2 has substrate specificity and inhibition characteristics distinct from those of indoleamine 2,3-dioxygenase-1. *Amino Acids* **2014**, *46*, 2155–2163. (b) D'Amato, N. C.; Rogers, T. J.; Gordon, M. A.; Greene, L. I.; Cochrane, D. R.; Spoelstra, S.; Nemkov, T. G.; D'Alessandro, A.; Hansen, K. C.; Richer, J. K. A TDO2-AhR signaling axis facilitates anoikis resistance and metastasis in triple-negative breast cancer. *Cancer Res.* **2015**, *75*, 4651–4664. (c) Merlo, L. M.; DuHadaway, J. B.; Grabler, S.; Prendergast, G. C.; Muller, A. J.; Mandik-Nayak, L. IDO2 modulates T cell-dependent autoimmune responses through a B cell-intrinsic mechanism. *J. Immunol.* **2016**, *196*, 4487–4497.

(15) (a) Weng, T.; Qiu, X.; Wang, J.; Li, Z.; Bian, J. Recent discovery of indoleamine-2,3-dioxygenase 1 inhibitors targeting cancer immunotherapy. *Eur. J. Med. Chem.* **2018**, *143*, 656–669. (b) Coletti, A.; Greco, F. A.; Dolciemi, D.; Camaioni, E.; Sardella, R.; Pallotta, M. T.; Volpi, C.; Orabona, C.; Grohmann, U.; Macchiarulo, A. Advances in indoleamine 2,3-dioxygenase 1 medicinal chemistry. *MedChemComm* **2017**, *8*, 1378–1392. (c) Prendergast, G. C.; Malachowski, W. P.; DuHadaway, J. B.; Muller, A. J. Discovery of IDO1 inhibitors: from bench to bedside. *Cancer Res.* **2017**, *77*, 6795–6811. (d) Röhrig, U. F.; Majjigapu, S. R.; Vogel, P.; Zoete, V.; Michielin, O. Challenges in the discovery of indoleamine 2,3-dioxygenase 1 (IDO1) inhibitors. *J. Med. Chem.* **2015**, *58*, 9421–9437. (e) Dounay, A. B.; Tuttle, J. B.; Verhoest, P. R. Challenges and opportunities in the discovery of new therapeutics targeting the kynurenine pathway. *J. Med. Chem.* **2015**, *58*, 8762–8782.

(16) (a) Balog, A.; Lin, T.-A.; Maley, E.; Gullo-Brown, J.; Hamza Kandoussi, E.; Zeng, J.; Hunt, J. T. Preclinical Characterization of Linrodostat Mesylate, a Novel, Potent, and Selective Oral Indoleamine 2,3-Dioxygenase 1 Inhibitor. *Mol. Cancer Ther.* **2020**, molcancer.0251.2020. (b) Yue, E. W.; Sparks, R.; Polam, P.; Modi, D.; Douthy, B.; Wayland, B.; Glass, B.; Takvorian, A.; Glenn, J.; Zhu, W.; Bower, M.; Liu, S.; Leffet, L.; Wang, Q.; Bowman, K. J.; Hansbury, M. J.; Wei, M.; Li, Y.; Wynn, R.; Burn, T. C.; Koblisch, H. K.; Fridman, J. S.; Emm, R.; Scherle, P. A.; Metcalf, B.; Combs, A. P. INCB24360 (Epcadostat), a Highly Potent and Selective Indoleamine-2,3-dioxygenase 1 (IDO1) Inhibitor for Immunoncology. *ACS Med. Chem. Lett.* **2017**, *8*, 486–491. (c) Soliman, H. H.; Antonia, S.; Sullivan, D.; Vanahanian, N.; Link, C. Overcoming coming tumor antigen energy in human malignancies using the novel indoleamine 2,3-dioxygenase (IDO) enzyme inhibitor, 1-methyl-D-tryptophan (1MT). *J. Clin. Oncol.* **2009**, *27*, 3004. (d) Kumar, S.; Waldo, J. P.; Jaipuri, F. A.; Marcinowicz, A.; Van Allen, C.; Adams, J.; Kesharwani, T.; Zhang, S.; Metz, R.; Oh, A. J.; Harris, S. F.; Mautino, M. R. Discovery of Clinical Candidate (1R,4r)-4-((R)-2-((S)-6-Fluoro-5H-imidazo[5,1-a]isoindol-5-yl)-1-hydroxyethyl)cyclohexan-1-ol (Navoximod), a Potent and Selective Inhibitor of Indoleamine 2,3-Dioxygenase 1. *J. Med. Chem.* **2019**, *62*, 6705–6733. (e) Crosignani, S.; Bingham, P.; Bottemanne, P.; Cannelle, H.; Cauwenberghs, S.; Cordonnier, M.; Dalvie, D.; Deroose, F.; Feng, J. L.; Gomes, B.; Greasley, S.; Kaiser, S. E.; Kraus, M.; Negrerie, M.; Maegley, K.; Miller, N.; Murray, B. W.; Schneider, M.; Solowej, J.; Stewart, A. E.; Tumang, J.; Torti, V. R.; Van Den Eynde, B.; Wythes, M. Discovery of a novel and selective

indoleamine 2,3-dioxygenase (IDO-1) inhibitor 3-(5-Fluoro-1H-indol-3-yl)pyrrolidine-2,5-dione (EOS200271/PF-06840003) and its characterization as a potential clinical candidate. *J. Med. Chem.* **2017**, *60*, 9617–9629.

(17) (a) Gangadhar, T. C.; Hamid, O.; Smith, D. C.; Bauer, T. M.; Waser, J. S.; Luke, J. J.; Balmanoukian, A. S.; Kaufman, D. R.; Zhao, Y.; Maleski, J.; Leopold, L.; Gajewski, T. F. Preliminary results from a phase I/II study of epcadostat (INCB024360) in combination with pembrolizumab in patients with selected advanced cancers. *J. Immunother. Cancer* **2015**, *3* (Suppl 2), 07. (b) A Phase 3 Study of Pembrolizumab + Epcadostat or Placebo in Subjects With Unresectable or Metastatic Melanoma (Keynote-252/ECHO-301). [ClinicalTrials.gov Identifier: NCT02752074](https://clinicaltrials.gov/ct2/show/study/NCT02752074). Last update: Sept. 4, 2019 (accessed on Oct. 23, 2019). (c) Long, G. V.; Dummer, R.; Hamid, O.; Gajewski, T.; Caglevic, C.; Dalle, S.; Arance, A.; Carlino, M. S.; Grob, J.-J.; Kim, T. M.; Demidov, L. V.; Robert, C.; Larkin, J. M. G.; Anderson, J.; Maleski, J. E.; Jones, M. M.; Diede, S. J.; Mitchell, T. C. Epcadostat (E) plus pembrolizumab (P) versus pembrolizumab alone in patients (pts) with unresectable or metastatic melanoma: Results of the phase 3 ECHO-301/KEYNOTE-252 study. 2018 ASCO Annual Meeting. *J. Clin. Oncol.* **2018**, *36*, 108. (suppl 15; abstr 108). (d) Sondak, V. K.; Khushalani, N. Y. Echoes of a failure: what lessons can we learn? *Lancet Oncol.* **2019**, *20*, 1037–1039. (e) Garber, K. A new cancer immunotherapy suffers a setback. *Science* **2018**, *360*, 588. (f) Komiya, T.; Huang, C. H. Updates in the clinical development of epcadostat and other indoleamine 2,3-dioxygenase 1 inhibitors (IDO1) for human cancer. *Front. Oncol.* **2018**, *8*, 423–429.

(18) Röhrig, U. F.; Reynaud, A.; Majjigapu, S. R.; Vogel, P.; Pojer, F.; Zoete, V. Inhibition Mechanisms of Indoleamine 2,3-Dioxygenase 1 (IDO1). *J. Med. Chem.* **2019**, *62*, 8784–8795.

(19) (a) Nelp, M. T.; Kates, P. A.; Hunt, J. T.; Newitt, J. A.; Balog, A.; Maley, D.; Zhu, X.; Abell, L.; Allentoff, A.; Borzilleri, R.; Lewis, H. A.; Lin, Z.; Seitz, S. P.; Yan, C.; Groves, J. T. Immune-modulating enzyme indoleamine 2,3-dioxygenase is effectively inhibited by targeting its apo-form. *Proc. Natl. Acad. Sci. U. S. A.* **2018**, *115*, 3249–3254. (b) Pham, K. N.; Yeh, S.-R. Mapping the Binding Trajectory of a Suicide Inhibitor in Human Indoleamine 2,3-Dioxygenase 1. *J. Am. Chem. Soc.* **2018**, *140*, 14538–14541.

(20) (a) A Study of Chemo Only Versus Chemo Plus Nivo With or Without BMS-986205, Followed by Post-Surgery Therapy With Nivo or Nivo and BMS-986205 in Patients With MIBC. [ClinicalTrials.gov Identifier: NCT03661320](https://clinicaltrials.gov/ct2/show/study/NCT03661320). (b) Sonpavde, G.; Necchi, A.; Gupta, S.; Steinberg, G. D.; Gschwend, J. E.; Van Der Heijden, M. S.; Garzon, N.; Ibrahim, M.; Raybold, B.; Liaw, D.; Rutstein, M.; Galsky, M. D. ENERGIZE: a Phase III study of neoadjuvant chemotherapy alone or with nivolumab with/without linrodostat mesylate for muscle-invasive bladder cancer. *Future Oncol.* **2020**, *16* (2), 4359–4368. (c) Taberner, J.; Luke, J. J.; Joshua, A. M.; Varga, A. L.; Moreno, V.; Desai, J.; Markman, B.; Gomez-Roca, C. A.; De Braud, F. G.; Patel, S. P. BMS-986205, an indoleamine 2,3-dioxygenase 1 inhibitor (IDO1i), in combination with nivolumab (NIVO): Updated safety across all tumor cohorts and efficacy in pts with advanced bladder cancer (advBC). *J. Clin. Oncol.* **2018**, *36*, 4512.

(21) Benarous, R.; Chevreuil, F.; Ledoussal, B.; Chasset, S.; Le Strat, F. Preparation of substituted thienylacetic acids as inhibitors of viral replication. WO 2014053666 A1. April 10, 2014.

(22) (a) Zhang, L.; Cherney, E. C.; Balog, A. J.; Zhu, X. Inhibitors of indoleamine 2,3-dioxygenase and methods of their use. WO 2018039518 A1; March 1, 2018. (b) Cherney, E. C.; Shan, W.; Zhang, L.; Nara, S. J.; Huang, A.; Balog, A. J. Inhibitors of indoleamine 2,3-dioxygenase and methods of their use. WO 2018039512 A. March 1, 2018.

(23) An Investigational Immuno-Therapy Study of Experimental Medication BMS-986242 Given in Combination With Nivolumab in Patients With Advanced Cancer. [ClinicalTrials.gov Identifier: NCT03351231](https://clinicaltrials.gov/ct2/show/study/NCT03351231).